Available online at www.sciencedirect.com
ScienceDirect
Journal of Photochemistry and Photobiology A: Chemistry 186 (2007) 270–277
Journal of Photochemistry and Photobiology A:Chemistry
www.elsevier.com/locate/jphotochem

Synthesis and photochemical investigations of novel bistriazene polyurethanes

Emil C. Buruiana [a,*], Violeta Melinte [a], Tinca Buruiana [a], Bogdan C. Simionescu [a,b], Thomas Lippert [c], Lukas Urech [c]

[a] *Petru Poni Institute of Macromolecular Chemistry, 700487 Iasi, Romania*
[b] *Department of Macromolecules, "Gh. Asachi" Technical University, 700050 Iasi, Romania*
[c] *Paul Scherrer Institut, 5232 Villigen PSI, Switzerland*

Received 14 June 2006; received in revised form 31 July 2006; accepted 18 August 2006
Available online 30 August 2006

Abstract

Two bistriazene monomers, 1,1′[4,4′-diphenyl]-3,3′-di(β-hydroxyethyl, methyl)-bistriazene (T1) and 1,1′[4,4′-diphenylsulfone]-3,3′-di(β-hydroxyethyl, methyl)-bistriazene (T2) were prepared by an electrophilic *N–N* coupling of substituted aryldiazonium salts with *N*-methyl-aminoethanol, and further employed as reaction partners for 2,4-toluene diisocyanate (2,4- and 2,6-TDI isomer mixture, 80:20, v/v) or 4,4′ methylene bis(phenylisocyanate) to achieve hard type bistriazene polyurethanes. The synthesized monomers and polymers were characterized by analytical and spectroscopic methods, while the surface morphology of polymers was visualized by scanning electron microscopy (SEM) and atomic force microscopy (AFM). Photochemical assessment of the triazene moieties in monomers and polymers was carried out in solution (methanol, DMF) and film state, following the decreasing under UV irradiation of the π–π^* absorption band in the corresponding UV spectra, the kinetic evaluation indicating a first order photoprocess. Laser ablation experiments performed at an irradiation wavelength of $\lambda = 308$ nm illustrate that bistriazene polyurethanes have a high potential to furnish good quality surfaces intended for microlithography.

Keywords: Bistriazene diol; Hard triazene polyurethanes; Photolysis; UV irradiation; Laser ablation

1. Introduction

Research on photopolymers in which photosensitive moieties are chemically incorporated has been motivated by various intriguing potential applications, the foremost of these including devices for optical data storage [1–3], photoresists [4–6] and photolithographic assemblies [7–9]. Such materials must be highly sensitive to light processing and should exhibit mechanical, thermal and chemical stability for all additional manufacturing steps. In this field, one of the most interesting topics in the recent years is the fabrication of artificial surface relief structures in triazene functionalized polymer films by their exposure to UV/laser irradiation, particularly attractive as dry etching of resists in microlithography [10–13]. Triazene polymers are suitable candidates for this type of applications owing to their high photosensitivity and especially spontaneous fragmentation into low molecular gaseous products upon irradiation [14]. Until now, a variety of triazene polymers, for instance polyesters [15], polytriazenes [16], polysulfides [17], have been obtained by different preparation methods and investigated from the point of view of the ablation properties.

Taking into account the broad spectrum of properties of the polyurethanes combined with a superior photosensitivity of triazene units, our group designed and synthesized a series of poly(ether urethanes) with such chromophore structures in the main backbone or as side chains introduced by means of new triazene monomers [18,19]. Studies performed on these systems revealed that materials photosensitivity increased with an increase of the triazene content in the polymers [20]. For this reason, new hard type triazene polyurethanes that include photolabile triazene units in every repeating segment were developed [21]. Excimer laser ablation experiments carried out on polyurethane films obtained from the latter polymers suggested a reduced quality of the ablation patterns as compared to other

* Corresponding author.
E-mail address: emilbur@icmpp.ro (E.C. Buruiana).

1010-6030/$ – see front matter © 2006 Elsevier B.V. All rights reserved.
doi:10.1016/j.jphotochem.2006.08.017

triazene polymers reported in the literature [22]. Therefore, the location of triazene units in the side chain of the polymeric backbone had a pronounced effect on the ablation parameters [23]. To surmount these limitations, a class of new hard triazene polyurethanes in which the photolabile units of bistriazene type are positioned in the polymer main chain was considered. This paper presents the synthesis, characterization and photochemical behaviour of these novel polymeric materials with a special emphasis on the photochemical and ablation properties.

2. Experimental

2.1. Materials

4,4′-Diaminodiphenyl, 4,4′-diaminodiphenyl sulfone, *N*-methyl-aminoethanol, toluene diisocyanate (2,4- and 2,6-TDI isomer mixture, 80:20, v/v) and 4,4′ methylene bis (phenylisocyanate) (Aldrich) were used as received. Dimethylformamide (DMF) wad dried over 5 Å molecular sieves.

2.2. Synthetic procedures

The bistriazene diols 1,1′[4,4′-diphenyl]-3,3′-di(β-hydroxyethyl, methyl)-bistriazene (T1) and 1,1′[4,4′-diphenylsulfone]-3,3′-di(β-hydroxyethyl, methyl)-bistriazene (T2) were synthesized in a two step procedure, as shown in Scheme 1. As an example, the synthetic pathway used to obtain the T1 monomer is described. A stirred solution of 4,4′-diamino-diphenyl (10 g, 0.054 mol) in HCl 10 wt.% (84 mL) was cooled to 0 °C and diazotized with an aqueous solution of sodium nitrite (7.5 g, 0.1 mol). The reaction mixture was dropwise added to a solution of N-methyl-aminoethanol (8.15 g, 0.1 mol) and sodium carbonate (9.1 g, 0.085 mol) in 250 mL water at 0 °C over 1 h. Then, 10 g sodium chloride was added and the resulting mixture was extracted three times with Et_2O. The organic layers were dried onto Na_2SO_4 and concentrated under reduced pressure. After removal of the solvent, the monomer was separated as a brown crystalline solid.

The hard type polyurethanes (PUH-T1 and PUH-T2) were obtained by polyaddition carried out in dry DMF starting from 5 g triazene diols and a corresponding stoichiometric amount of toluene diisocyanate (2,4- and 2,6-TDI isomer mixture, 80:20, v/v) (PUH-T1) or 4,4′ methylene bis(phenylisocyanate) (PUH-T2). The reactions were performed under purified nitrogen at 65 °C for 15 h. The triazene polyurethanes were precipitated in methanol and dried for 48 h at 60 °C under reduced pressure.

2.3. Equipment

The polymer structures were verified by ^{1}H NMR, IR and UV spectroscopy using a Bruker 400 MHz spectrometer, a Specord M80 and a Specord M42 spectrophotometer, respectively. Gel permeation chromatography (GPC) measurements were determined with a PL MD-950 instrument (Polymer Laboratories) equipped with an evaporative mass detector and two PL gel 5 μm columns. The sample for measurement was 1.0 g dL^{-1} solution in DMF and the flow rate of the carrier solvent was 1 mL min^{-1}. The average molecular weight was calculated on the basis of the molecular weight versus retention volume curve of monodisperse polystyrene standard. The thermal stability of the polyurethanes was analyzed through thermogravimetry using a MOM Budapest derivatograph. TG and TGA curves were recorded between 20 and 600 °C with a heating rate of 12 °C min^{-1} in air. UV irradiations were performed in DMF solutions and for thin films, using a 500 W high-pressure mercury lamp without wavelength selection, at room temperature. The initial absorbance of the samples in the absorption band maximum was kept between 0.9 and 1.0. For the irradiation at 308 nm a Complex 205 XeCl excimer laser from Lambda Physik (τ = 30 ns) was used. The samples for the laser ablation experiments were prepared by solvent casting from a 15 wt.% DMF solution on glass substrates. SEM analyses were made through polymer film deposition on aluminum plates and subsequent metallization with gold layer. AFM measurements of the samples were achieved in air at room temperature, using a PicoScan (Molecular Imaging) system, with a scanning area of 30 μm.

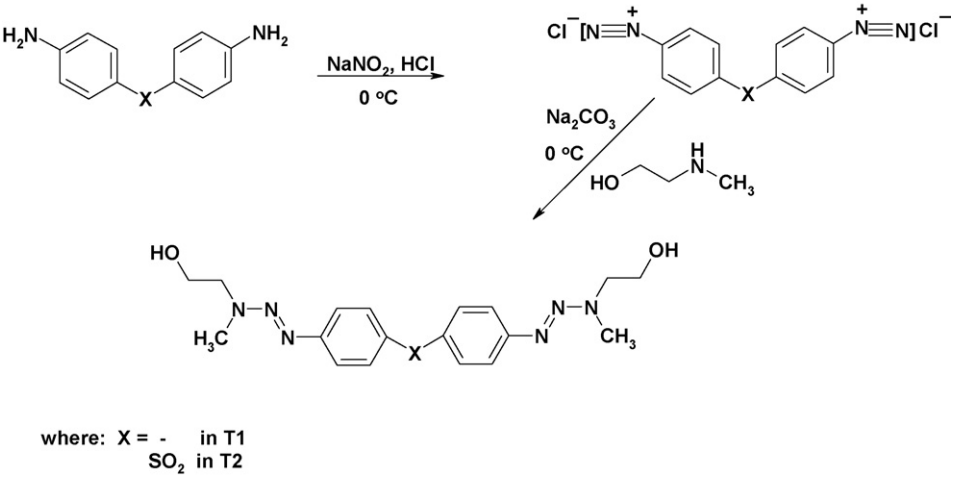

Scheme 1. Synthesis of bistriazene monomers (T1 and T2).

2.4. Measurements

2.4.1. 1,1′[4,4′-diphenyl]-3,3′-di(β-hydroxyethyl, methyl)-bistriazene (T1)

Elem. Anal. Calcd. for $C_{18}H_{24}N_6O_2$: C, 60.67%; H, 6.74 %; N, 23.59%. Found: C, 60.48%; H, 6.71%; N, 23.65%.

^{1}H NMR [$CDCl_3$, δ ppm]: 7.57 (d, 4H, $J = 8$ Hz, aromatic protons in *ortho* position towards triazene groups); 7.48 (d, 4H, $J = 8$ Hz, aromatic protons in *meta* position relative to triazene groups); 3.89 (s, 8H, –N–C$\underline{H_2}$–C$\underline{H_2}$–OH); 3.35 (s, 6H, N-CH_3); 2,84 (m, 2H, OH).

IR (KBr, cm^{-1}): 3390 (OH); 2900 (CH_2 asymmetric); 2845 (CH_2 symmetric); 1550 and 840 (CH aromatic); 1360 (N=N–N<); 1240, 1200 and 1100 (C–O).

UV (CH_3OH): 360 nm. Yield: 8.85 g (81%).

2.4.2. 1,1′[4,4′-diphenylsulfone]-3,3′-di(β-hydroxyethyl, methyl)-bistriazene (T2)

Elem. Anal. Calcd. for $C_{18}H_{24}N_6O_4S$: C, 51.42%; H, 5.71%; N, 20%. Found: C, 51.50%; H, 5.83%; N, 19.85%.

^{1}H NMR ($CDCl_3$, δ ppm): 7.95 (d, 4H, $J = 8$ Hz, aromatic protons in *ortho* position to triazene groups); 7.39 (d, 4H, $J = 8$ Hz, aromatic protons in *meta* position relative to triazene groups); 3.95 (s, 8H, –N–C$\underline{H_2}$–C$\underline{H_2}$–OH); 3.34 (s, 6H, N-CH_3); 2.9 (m, 2H, OH).

IR (KBr, cm^{-1}): 3350 (OH); 2930 (CH_2 asymmetric); 2855 (CH_2 symmetric); 1600 and 850 (CH aromatic); 1370 (N=N–N<); 1240, 1200 and 1100 (C–O).

UV (CH_3OH): 342 nm. Yield: 9.13 g (86%).

2.4.3. PUH-T1

Elem. Anal. Calcd. for $[C_{27}H_{30}N8O_4]_n$: C, 61.13%; H, 5.66%; N, 21.13%. Found: C, 60.97%; H, 5.70%; N, 21.16%.

^{1}H NMR (DMSO-d_6, δ ppm): 9.6 (m, NH-COO); 7.4–7.9 (m, aromatic protons from TDI and T1 monomer); 4.45 (m, NHCOO–CH_2–CH_2); 4.1 (m, NHCOO–C$\underline{H_2}$–CH_2–N(CH_3)–N=N); 3.67 (s, –N(CH_3)–N=N<), 1.98–2.18 (m, Ph-C$\underline{H_3}$).

IR (KBr, cm^{-1}): 3350 (NH); 2900 (CH_2); 1720 (C=O free); 1600 and 820 (CH aromatic); 1360 (N=N–N<); 1220, 1100 (O–C–O).

UV (DMF): 355 nm.

2.4.4. PUH-T2

ELEM. Anal. Calcd. for $[C_{33}H_{34}N_8O_6S]_n$: C, 59.10%; H, 5.07%; N, 16.71%. Found: C, 59.06%; H, 5.09%; N, 16.69%.

^{1}H NMR (DMSO-d_6, δ ppm): 9.5 (m, N$\underline{H}$-COO); 7.05–7.85 (m, aromatic protons from MDI and T2 monomer); 4.37 (m, NHCOO–C$\underline{H_2}$–CH_2); 4.1 (m, NHCOO–C$\underline{H_2}$–CH_2–N(CH_3)–N=N); 3.67 (s, Ph-C$\underline{H_2}$-Ph); 3.23 (s, –N(CH_3)–N=N<).

IR (KBr, cm^{-1}): 3325 (NH); 2910 (CH_2); 1675 (C=O free); 1600 (CH aromatic); 1525 (NH); 1360 (N=N–N<).

UV (DMF): 344 nm.

3. Results and discussion

The preference for a bistriazene derivative characterized by a rich conjugation over the π electrons from triazene unit and the π electrons subsequently to the aromatic rings is motivated by a possible increase of chromophore photostability in such structures, with significant effect on their laser ablation behaviour. Therefore, two new bistriazene diols (T1, T2) were synthesized by *N–N* coupling of the aromatic diazonium salt with *N*-methylaminoethanol, according to Scheme 1. The structure and purity of T1 and T2 was confirmed by IR, ^{1}H NMR and UV spectroscopy, as well as by elemental analysis. For example, Fig. 1 shows the ^{1}H NMR spectrum of T1 diol, where the doublet peak at 7.48 ppm is assigned to the aromatic protons in *meta* position related to the triazene group, and the peak at 7.57 ppm is determined of the aromatic protons in *ortho* position (for details, see Section 2). Due to the complementarities of the protons in the spectra of both monomers appear the same signals, the only difference being caused by the integral intensities. Additionally, in the case of T2 a small shift of the signal at 7.39 and 7.95 ppm owing to the aromatic protons in *meta* and *ortho* position to the triazene groups was noticed as result of the presence of the sulfone group between the two aromatic rings. Concerning the ethylene protons, we do not observe different chemical shifts, since they are equivalent, a similar result being evidenced on triazene alcohol derivatives [15,20]. The integrals ratio of aliphatic versus aromatic protons sustains the proposed structure of the bistriazene diols.

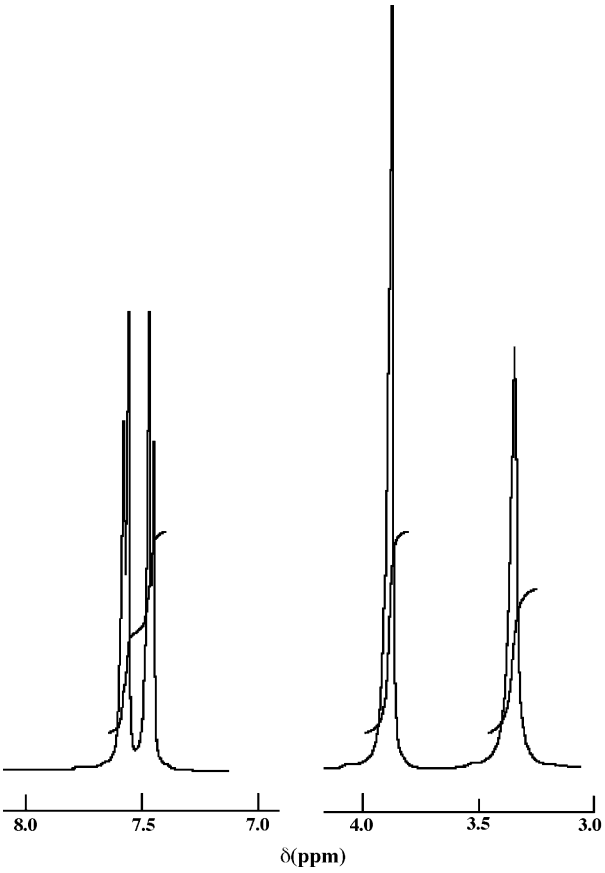

Fig. 1. ^{1}H NMR spectrum of T1 bistriazene diol in chloroform.

For the purpose of obtaining of materials microstructured by UV/laser irradiation, the effect of triazene structure on the photosensitivity of polymers was further examined. In this context,

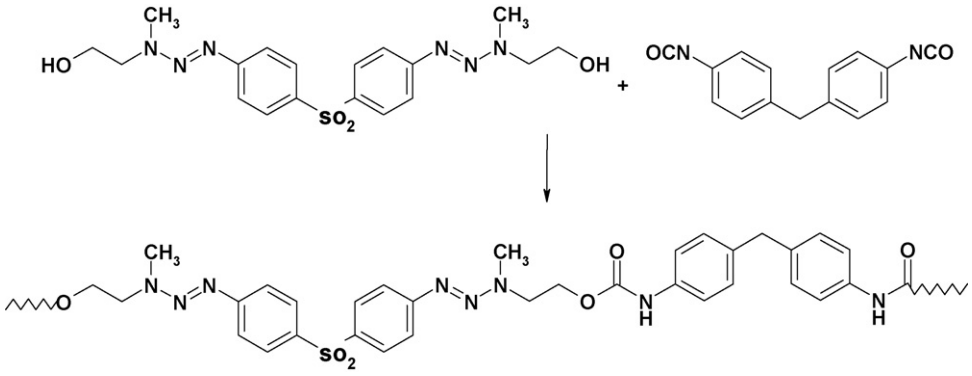

Scheme 2. Synthesis of bistriazene polyurethane PUH-T2.

two new hard polyurethanes (PUH-T1 and PUH-T2), resulted by the reaction between a diisocyanate (2,4 toluene diisocyanate or 4,4′ methylene bis(phenylisocyanate) and a bistriazene diol, were synthesized and studied. Scheme 2 depicts the synthetic pathway used to obtain the hard triazene polyurethane PUH-T2.

As in the case of monomers, the structure of bistriazene polyurethanes was confirmed by elemental analysis and spectral methods. The IR spectra of polymers contain besides specific absorption bands assigned to triazene monomer, the bands introduced by the urethane sequences. Fig. 2 illustrates the ^{1}H NMR spectrum of PUH-T1 polyurethane for a comparison with the bistriazene monomer T1 (spectrum given in Fig. 1). The multiplet centred at 2.08 ppm was attributed to the protons included in the CH_3 unit attached to the aromatic ring from 2,4- and 2,6-toluene diurethanes, whereas the other aliphatic protons from the alkyl chain of the bistriazene appeared as a singlet at 4.1 ppm (NHCOO–CH_2–C$\underline{H_2}$–N(CH_3)–N=N) and at 4.45 ppm (NHCOO–CH_2–CH_2). The protons from methyl units in the neighbourhood of the triazene moieties provide two singlets at 3.67 and 3.83 ppm. The aromatic protons generated through the reaction of bistriazene diol and diisocyanate give a multiplet signal situated between 7 and 7.96 ppm, and that of the NH group appears as multiplet at 9.6 ppm.

Compared to monomers, the methylene protons in polymers appear as two signals shifted with about 0.11 and 0.56 ppm (PUH-T1), and respectively, 0.15 and 0.42 ppm (PUH-T2) as result of the formation of urethane structures, whose protons resonate at a downfield induced by the deshielding effect of urethane group.

The synthesized bistriazene polyurethanes present good solubility in common polyurethane solvents (DMF and DMSO), as well as excellent film forming properties, so that homogeneous and transparent yellow films were easily prepared by solvent casting with subsequent drying at moderate temperature. The molecular weights of the polymers determined by GPC were below 10,000.

A representative feature of the triazene polyurethanes is their thermal behaviour, which may have direct consequences over their applicability in microlithography or as macroinitiators in preparing of various materials. To establish a correspondence between the polymer structure and the content of triazene moieties in the polymeric backbone, thermogravimetric analysis was used, the data being presented in Table 1. As can be observed, the thermal stability of bistriazene polyurethanes is relatively low, as compared to that of elastomeric polyurethanes, as an outcome of the increased amount of triazene units in polymer.

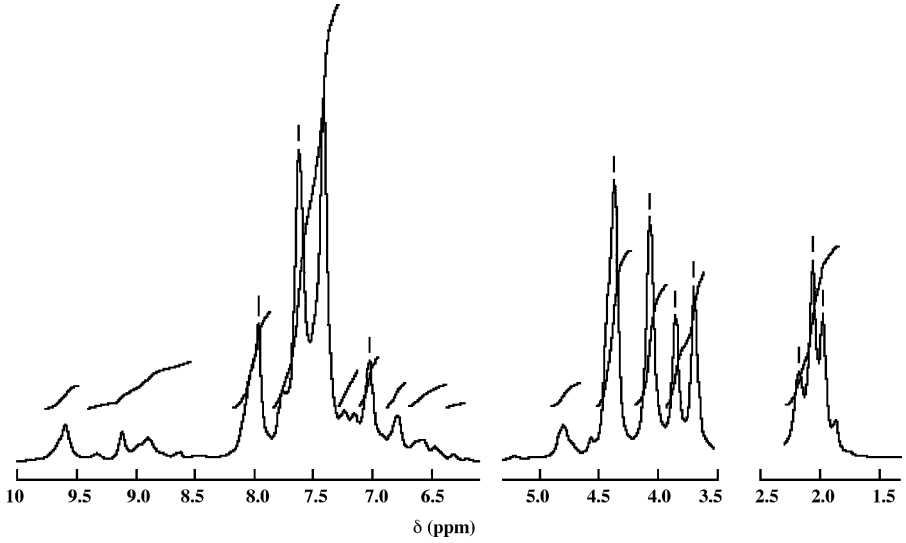

Fig. 2. ^{1}H NMR spectrum of bistriazene polyurethane PUH-T1 in DMSO-d_6.

Table 1
Thermal behaviour of bistriazene polyurethanes

Sample	Stage I			$T_{10\%}$ (°C)	Stage II			Stage III		
	$T_I - T_f$ (°C)	T_{max} (°C)	Weight loss (%)		$T_I - T_f$ (°C)	T_{max} (°C)	Weight loss (%)	$T_I - T_f$ (°C)	T_{max} (°C)	Weight loss (%)
PUH-T1	90–175	140	16	150	175–240	205	8	240–360	325	15
PUH-T2	110–190	150	12	175	190–255	220	11	280–430	375	18

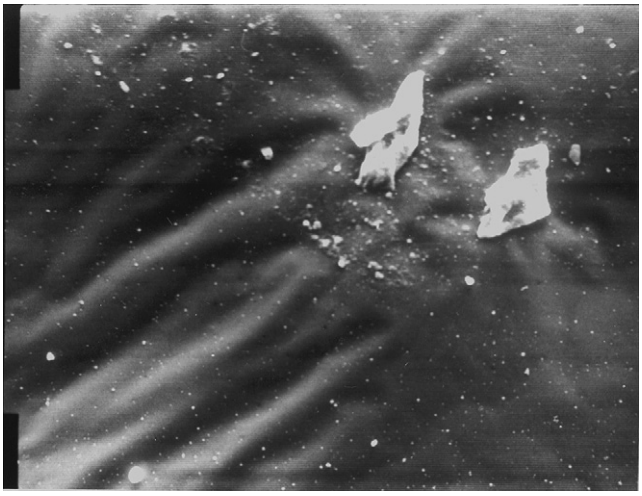

Fig. 3. SEM micrographs of the bistriazene polyurethane PUH-T2 at 2300×.

In agreement with literature data, a higher amount of photolabile chromophore in polymers had as effect a decrease of the thermal stability of the triazene polymers [24]. Technically, the weight loss observed in the first stage of the process is attributed to the triazene unit decomposition that releases small volatile molecules such as nitrogen, followed by the thermal decomposition of polymeric backbone.

The surface topography of the bistriazene polyurethanes was examined by scanning electron microscopy (SEM) and atomic force microscopy (AFM). Fig. 3 displays the SEM micrograph of bistriazene polyurethane (PUH-T2), where a homogenous morphology is clearly evidenced, as a consequence of the unitary structure of the hard polyurethane. AFM investigations were made in the bottom of the polymer surfaces as well as on the top, with a scanning area of 3 μm × 3 μm or 30 μm × 30 μm. Fig. 4(a) shows a schematic representation of the polyurethane morphology in thin film suggesting the same homogeneous structure of the polymer. Although PUH-T2 had a good-quality

Table 2
Physical and photolysis data of bistriazene monomers and polymers

Sample	λ_{max} (nm)		k (10^{-4} s^{-1})		Time (min)	
	Solution	Film	Solution	Film	Solution	Film
T1	360		5.3		50	
T2	342		6.8		35	
PUH-T1	355	352	9.26	11.3	42	9
PUH-T2	344	342	2.5	5.7	51	12

film its surface is not flat and clean resulting in numerous hills and valleys placed into a smooth structure, this image seems to suggest the presence of crystallites at bottom with size below 100 nm.

As already reported [14], the choice of triazene chromophore is mainly stimulated by the opportunity to correlate its absorption maximum in the UV spectrum with laser radiation wavelength. The most profitable way is including of suitable substituents in the vicinity of the triazene group from polymer backbone. In our case, the triazene chromophore presents in the UV spectra a broad absorption maximum, attributed to π–π^* transitions, centred at 360 nm for T1 monomer, while the T2 diol has an absorption peak at 342 nm. Under UV irradiation, the triazene group is decomposed with the release of small gaseous molecules (N_2, CO_2)—process reflected in the UV spectra by a decreasing of the absorption maximum. The monitoring of this photobehaviour with irradiation time allows an estimation of the rate and photodecomposition degree for the triazene chromophore (Table 2).

The photochemical response of bistriazene derivatives was studied in methanol solution by exhaustive UV irradiation with a high pressure mercury lamp. Fig. 5 illustrates the diminishing of the absorption maximum in the UV spectrum of T1 bistriazene diol with the irradiation time. It was noticed that the absorption maximum is decreasing with the irradiation time up to a limit, when it is supposed that all triazene units are decom-

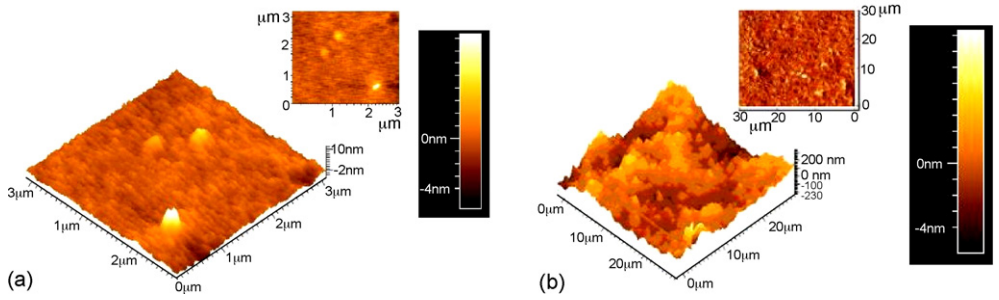

Fig. 4. AFM topography images for polymeric films based on bistriazene polyurethanes: PUH-T1 (a) and PUH-T2 (b).

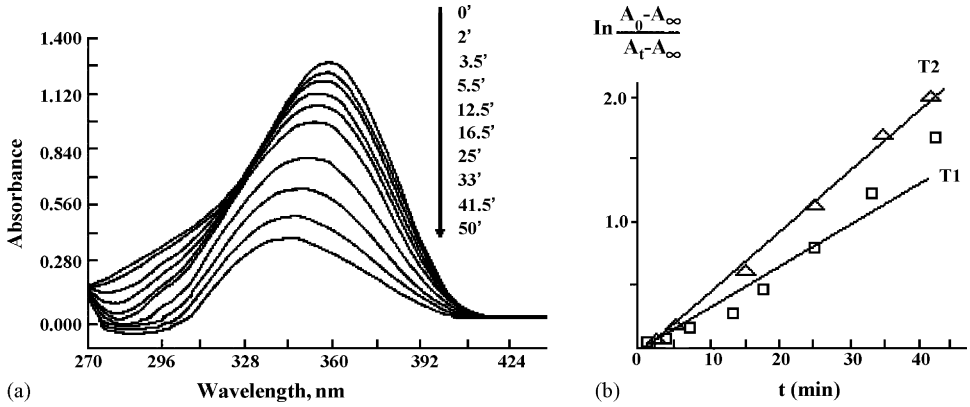

Fig. 5. UV–vis spectrum of bistriazene monomer T1 in methanol solution monitoring the vanishing of the UV absorption maximum of the triazene linkage after different irradiation periods (plot a), and kinetic evaluation of the photolysis of T1 monomer (□) and T2 monomer (△), respectively (plot b) at 298 K.

posed and UV absorption tends to zero. The photodecomposition of biphenyl bistriazene monomer in methanol was completed within about 50 min, with a kinetic rate $k = 5.3 \times 10^{-4}\ s^{-1}$, a time period longer than in the case of diphenylsulfone bistriazene where the same process took place in about 35 min ($k = 6.8 \times 10^{-4}\ s^{-1}$). Furthermore, the existence of isosbestic points at 270 and 425 nm for T1 and at 250 and 430 nm in T2 clearly indicates that the photoreaction proceeds uniformly. This result may be evaluated by means of the photocleaving reaction of triazene groups, induced of interaction with UV light. The first part of the photolysis of biphenyl bistriazene derivative proceeds with a slow diminising of the photodecomposition rate, followed in the second stage by an increase, suggested that beyond the breakage of triazene linkage, the molecular conjugation is interrupted with consequences over the dynamical evolution of the ablation. Compilation of this result with those achieved for biphenylsulfone bistriazene illustrates that the photosensitivity of the triazene moiety rigorously depends on conjugation effects generated by the nature of the substituents in the chromophore neighborhood. This peculiarity is confirmed by constant rate values, determined from the kinetic curves of the studied monomers (Fig. 5b). The photochemical ablation of triazene monomers is quantitatively described through a constant rate value, given by the expression:

$$k = \ln \frac{A_0 - A_\infty}{A_t - A_\infty} \frac{1}{t} \quad (1)$$

where A_0, A_t and A_∞ are the values of the absorbance at time 0, t and ∞, respectively. The kinetic representation obtained by plotting the logarithm of the reduced absorption against time indicates a first-order kinetic of the photoprocess. As the kinetic slope is higher, the photodecomposition process is faster and as a consequence, the bistriazene compound presents a high photosensitivity.

The photolytic estimation of the triazene units in polyurethanes was performed by UV irradiation in DMF solutions and film state. By exposing PUH-T1 solution to UV irradiation, a gradual decrease of the absorption maximum centered at 355 nm with the irradiation period was detected (Fig. 6a). In the case of PUH-T1 polyurethane the rate constant is $k = 9.26 \times 10^{-4}\ s^{-1}$ and the photodecomposition of the triazene group is accomplished in 42 min in particular experimental conditions. In identical circumstances, the PUH-T2 polymer presents a similar behaviour, with $k = 2.5 \times 10^{-4}\ s^{-1}$ and a total vanishing of the absorption maximum in about 51 min. Such results illustrate minimum differences between the above

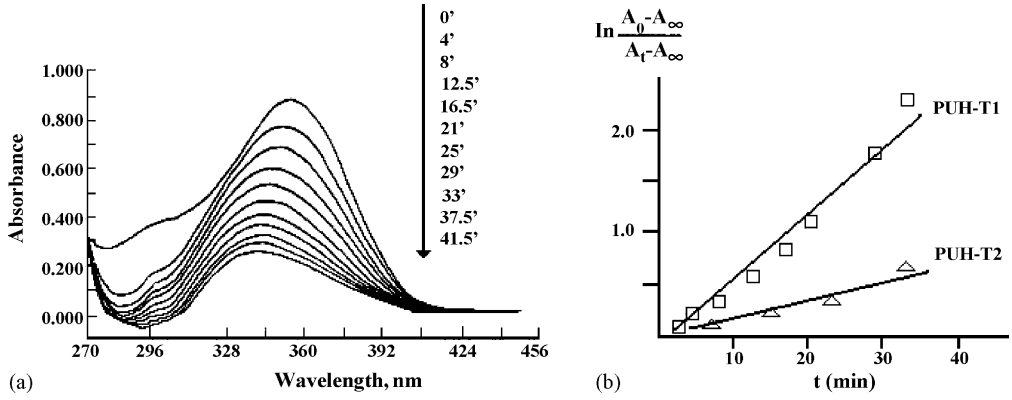

Fig. 6. The photolytic behaviour of the PUH-T1 polymer in DMF solution (plot a) and the kinetic evaluation of its photolysis (plot b) (□) as compared to that of the PUH-T2 polyurethane (△).

discussed polyurethanes, probably due to the structural resemblance of the bistriazene chromophores.

The photochemical behaviour of the bistriazene polyurethanes in film state represents a major feature required by dry etching applications. For this, the polymeric films were subjected to UV irradiation, to establish their ability to function as photolithographic materials. The photolytic degradation of PUH-T1 film proceeds in 9 min with a rate constant $k = 11.38 \times 10^{-4}\,s^{-1}$, whereas for PUH-T2 film the photodecomposition of the bistriazene groups took place in 12 min, the rate constant being $k = 5.7 \times 10^{-4}\,s^{-1}$. The comparison of the results obtained in film state with those corresponding to polymer solution, irradiation revealed that the photosensitivity of bistriazene groups is superior in polymeric films. A reasonable explanation is offered by the steric hindrance apparent in the polymer backbone, or to the potential recombination of the macroradicals generated in solvent cage, before deactivation.

In addition to UV investigations, the bistriazene polyurethane films were subjected to laser irradiation, to evaluate the influence of laser beam on polymer surface. A great advantage of laser ablation comes from its wavelength selectability, which may be adjusted to chromophore UV absorption in order to achieve promising materials for microlithographic purposes. The polymeric films were prepared by spin-coating on quartz substrates. The laser ablation properties, i.e. threshold fluence, ablation rate and quality were studied as a function of the laser fluence.

The description of the ablation phenomenon is given by a linear relation connecting the ablation parameters:

$$d(F) = \frac{1}{\alpha_{\text{eff}}} \ln\left(\frac{F}{F_{\text{th}}}\right) \quad (2)$$

where $d(F)$ is the ablated depth per pulse, F the laser fluence, F_{th} the threshold fluence and α_{eff} is the effective ablation coefficient.

In the present study, it was found that the hard triazene polyurethane PUH-T1 provides a threshold fluence of 83 mJ cm^{-2} and an effective absorption coefficient for ablation of 14.874 cm^{-1}, whereas for the second polyurethane in the low fluence range a threshold fluence of 59 mJ cm^{-2}, and α_{eff} of 18.739 cm^{-1} were determined. The plot of the etch rate versus fluence, shown in Fig. 7, gives a linear dependence which indicates no incubation behaviour, as expected for highly absorbing

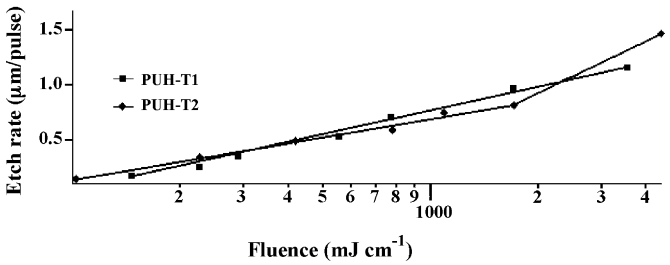

Fig. 7. Plot of the etch rate vs. fluence of hard bistriazene polyurethanes.

Table 3
Ablation parameters of bistriazene polyurethanes

Sample	α_{eff} (cm^{-1})	F_{th} (mJ)	$\alpha_{\text{lin (308 nm)}}$ (cm^{-1})
PUH-T1	14,874	82.9	29,050
PUH-T2	18,739	59.3	20,041
PU-NO[a]	40,000	52	10,400

[a] Ref. [21].

polymers. For lithographic applications, the low fluence range (between 10 and 400 mJ cm^{-2}) offers the opportunity to study the influence of structural parameters on the ablation rates.

The measured linear absorption coefficients (α_{lin}) of the polyurethanes are higher than the values of the α_{eff} calculated from relation (2), the differences being due to the decomposition of the triazene unit during the laser pulse [25]. The quality of the structure and the resolution at 308 nm were illustrated by scanning electron microscopy. Fig. 8 exemplifies the corners of the ablation holes in PUH-T1 (a) and PUH-T2 (b) made after two pulses at 1700 mJ cm^{-1} and four pulses at 4400 mJ cm^{-1}, respectively. It can be remarked that no debris originating from expelled fragments is visible, and the consequent edges are straight, sharp and without damage. These sustain a well defined structuring process mainly due to the decomposition of the triazene moieties. By estimates from the size of the microridges, the resolution is, as expected, in the micrometer or even submicrometer domain. As compared to other triazene polyurethanes previously studied [21], bistriazene polymers provide enhanced ablation characteristics, mostly due to the different architecture of the present polyurethanes, which confirm the literature data [23] revealing that microstructures made in main-chain polymers show higher quality than those in the pending sys-

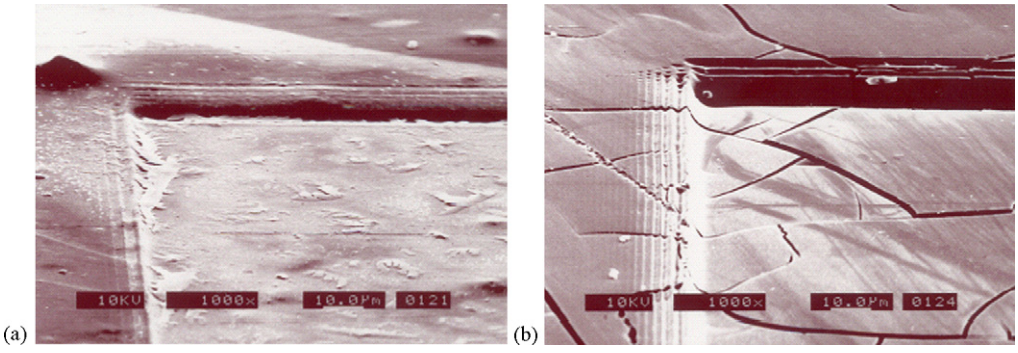

Fig. 8. SEM micrographs of the ablation holes (308 nm) in PUH-T1 after two pulses at 1700 mJ cm^{-2} (a) and PUH-T2 after four pulses at 4400 mJ cm^{-2} (b) evidencing the resolution and the well-defined patterning of the polymeric surface.

tems, whereas the characteristic data of ablation are quite similar (Table 3). Additional investigation of the bistriazene hard polyurethanes exposed to UV/laser irradiation is in progress.

4. Conclusions

New photolabile bistriazene monomers were synthesized and characterized. Polyaddition reaction between bistriazene diols and diisocyanates yielded photopolymers with triazene-bridges in the backbone, which are the most appropriate systems for UV/laser photolithography. Significant photolytic sensitivity was detected by irradiating and monitoring the polyurethanes through UV spectroscopy in defined intervals. The experiments performed with the excimer laser (308 nm) demonstrated that the designed bistriazene polymers could be used for the fabrication of microstructures with adequate precision. Consequently, the generated microridges illustrate the absence of any amount of redeposited material on edges and the achieving of a very smooth surface. Thus, such bistriazene polymers seem to be suitable for applications with stringent ablation characteristics.

Acknowledgment

E.C.B. expresses his gratitude to the National University Research Council (MEC-CNCSIS) that financially sustained this work through Grant 32952/2005.

References

[1] A. Natansohn, P. Rochon, Chem. Rev. 102 (2002) 4139.
[2] T.J. Trentler, J.E. Boyd, V.L. Colvin, Chem. Mater. 12 (2000) 1431.
[3] I. Gourevich, H. Pham, J.E.N. Jonkman, E. Kumacheva, Chem. Mater. 16 (2004) 1472.
[4] P. Gupta, S.R. Trenor, T.E. Long, G.L. Wilkes, Macromolecules 37 (2004) 9211.
[5] J.M. Havard, S.-Y. Shim, J.M.J. Frechet, Chem. Mater. 11 (1999) 719.
[6] A.W. Harant, V.S. Khire, M.S. Thibodaux, C.N. Bowman, Macromolecules 39 (2006) 1461.
[7] P.S. Ramnujam, N.C.R. Holme, M. Petersen, S. Hvilsted, J. Photochem. Photobiol. A: Chem. 145 (2001) 49.
[8] R. Michel, J.W. Lussi, G. Csucs, I. Reviakine, G. Danuser, B. Ketterer, J.A. Hubbell, M. Textor, N.D. Spencer, Langmuir 18 (2002) 3281.
[9] K. Morigaki, H. Schőnherr, C.W. Frank, W. Knoll, Langmuir 19 (2003) 6994.
[10] O. Nuyken, C. Scherer, A. Baindl, A. Brenner, U. Dahn, R. Gartner, S. Kaiser-Rohrich, R. Kollefrath, P. Matusche, B. Voit, Prog. Polym. Sci. 22 (1997) 93.
[11] T. Lippert, M. Hauer, C. Phipps, A. Wokaun, High-power laser ablation, in: C.R. Phipps (Ed.), Proceedings of the SPIE, 2002, pp. 63–71.
[12] T. Lippert, C. David, M. Hauer, A. Wokaun, J. Robert, O. Nuyken, C.R. Phipps, J. Photochem. Photobiol. A: Chem. 145 (2001) 87.
[13] T. Lippert, M. Hauer, C.R. Phipps, A. Wokaun, Appl. Phys. A 77 (2003) 259.
[14] T. Lippert, J.T. Dickinson, Chem. Rev. 103 (2003) 453.
[15] O. Nuyken, U. Dahn, J. Polym. Sci., Part A: Polym. Chem. 35 (1997) 3017.
[16] J. Stebani, O. Nuyken, T. Lippert, A. Wokaun, Makromol. Chem., Rapid. Commun. 14 (1993) 365.
[17] O. Nuyken, U. Dahn, W. Ehrfeld, V. Hessel, K. Hesch, J. Laudsiedel, J. Diebel, Chem. Mater. 9 (1997) 485.
[18] E.C. Buruiana, V. Niculescu, T. Buruiana, J. Appl. Polym. Sci. 88 (2003) 1203.
[19] E.C. Buruiana, V. Niculescu, T. Buruiana, J. Appl. Polym. Sci. 92 (2004) 2599.
[20] E.C. Buruiana, V. Melinte, T. Buruiana, B.C. Simionescu, J. Appl. Polym. Sci. 96 (2005) 385.
[21] E.C. Buruiana, V. Melinte, T. Buruiana, T. Lippert, H. Yoshikawa, H. Mashuhara, J. Photochem. Photobiol. A: Chem. 171 (2005) 261.
[22] J. Wei, T. Lippert, N. Hoogen, O. Nuyken, A. Wokaun, J. Phys. Chem. B 105 (2001) 1267.
[23] O. Nuyken, U. Dahn, A. Wokaun, T. Kunz, C. Hahn, V. Hessel, J. Laudsiedel, Acta Polym. 49 (1998) 427.
[24] N. Hoogen, O. Nuyken, J. Polym. Sci. Part A: Polym. Chem. 38 (2000) 1903.
[25] T. Lippert, L.S. Bennet, T. Nakamura, H. Niino, A. Ouchi, A. Yabe, Appl. Phys. A: Mater. Sci. Process. 63 (1996) 257.